

Xu Yifei (Orcid ID: 0000-0002-6907-1187)

Islam Abu Reza Md. Towfiqul (Orcid ID: 0000-0001-5779-1382)

Effects of cyclic variability in Pacific decadal oscillation on winter wheat production in China

Yifei Xu¹, Te Li², Shuanghe Shen^{1,*}, Guodong Xu³, Abu Reza Md. Towfiqul Islam⁴, Zhenghua Hu^{1,*}

1 School of Applied Meteorology, Collaborative Innovation Center on Forecast and Evaluation of Meteorological Disasters and Key Laboratory of Meteorological Disaster of Ministry of Education, Nanjing University of Information Science & Technology, Jiangsu Nanjing 210044

2 School of Atmospheric Sciences and Institute for Climate and Global Change, Nanjing University, Jiangsu Nanjing 210023

3 Prevention Technology Center on Meteorological Disasters, Heze Meteorological Bureau, Shandong Heze 274000

4 Department of Disaster Management, Disaster Management E-Learning Centre, Begum Rokeya University, Rangpur 5400, Bangladesh

Co-author: Te Li

Submitted

Supported by the China Meteorological Administration Special Public Welfare Research Fund (GYHY201506001)

Abstract

Due to restrictions on the long period ranges of Pacific decadal oscillation (PDO) and the limited amount of winter wheat yield data in China, there is little knowledge or understanding of the effects of PDO on winter wheat production in China. To fill this knowledge gap, we simulated over one hundred years of winter wheat yields using a process-based crop model over eight locations in the dominant winter wheat-producing area across China during 1902–2014. By using the continuous wavelet transform (CWT), we found that winter wheat yields had inter-annual variability (4- and 8-year periods) and interdecadal oscillations (22-year and over 50-year). The cross wavelet transform (XWT) results indicated that interdecadal variations of winter wheat yields and PDO were in

This article has been accepted for publication and undergone full peer review but has not been through the copyediting, typesetting, pagination and proofreading process which may lead to differences between this version and the [Version of Record](#). Please cite this article as doi: [10.1002/joc.6956](https://doi.org/10.1002/joc.6956)

This article is protected by copyright. All rights reserved.

phase. The interdecadal variation components of PDO and winter wheat yields from 1902 to 2014 show that when PDO was in the positive (negative) phase, winter wheat yields tended to increase (decrease) by using the ensemble empirical mode decomposition (EEMD) method. The interdecadal variations of winter wheat yields were significantly associated with PDO and the mean correlation coefficient was 0.83. The contribution rate of PDO on winter wheat yields was approximately 11%. The interdecadal variation in winter wheat production was principally determined by the interdecadal oscillation in April precipitation and December temperature, which was modulated by the phase change of PDO. The mean correlation coefficient was -0.50 and 0.59, respectively. This is because during the negative (positive) phase of PDO, more (less) April precipitation and lower (higher) December temperature in the study area occur, whereas an increase in April precipitation and lower December temperature adversely affect winter wheat production. This study can aid governments and farmers to recognize the hazards of excess April precipitation and low December temperature in negative PDO years. Overall, the decadal variation in winter wheat yields due to PDO facilitates the prediction of winter wheat yields, and PDO influences crop growth by modulating large-scale oscillation patterns.

Keywords: PDO, interdecadal variability, winter wheat, crop yield.

1 Introduction

The climate variation has significant impacts on crop production and increases risk in crop management (Nicholls, 1997; Hoogenboom, 2000; Rosenzweig et al., 2001; Ren et al., 2019). A substantial body of literature in China describes research into the effects of climate change on winter wheat production and crop yields (Song et al., 2019; Ren et al., 2019; Huang et al., 2020). Recent studies have focused on the teleconnections between large-scale climate patterns and crop management (Li et al., 2020; Tian et al., 2015; Brown, 2013; Jarlan et al., 2014; Iizumi et al., 2014; Maxwell et al., 2013; Shuai et al., 2013, 2016). For instance, Shuai et al. (2013) pointed out that El Niño-Southern Oscillation (ENSO) has significant impacts on wheat yields, and more rainfall in El Niño

years leads to a decrease in wheat yields. Climate indices have serious impacts on flood-induced agricultural loss across China. Zhang et al. (2016) demonstrated that ENSO could be taken as a suitable predictor for flood-affected and flood-destroyed crop areas across China. Significant influences of Pacific decadal oscillation (PDO) and the North Atlantic Oscillation (NAO) events on agricultural floods are identified mainly in the coastal provinces of southeast China; while in central China, cold Atlantic Multidecadal Oscillation (AMO) and cold NAO tend to influence flood-affected and flood-destroyed crop areas in coastal provinces of east China. Studies into the effects of large-scale teleconnections on local climate will be conducive to improving crop management (Baigorria, 2008; Bannayan, 2010). Previous studies have mainly focused on the impacts of ENSO or several climate signals on crop management (Shuai et al., 2013, 2016), but normally in recent decades. It should be noted here that the teleconnection between multidecadal climate patterns and crop management can potentially improve future predictions of crop yield risks (Tian et al., 2015), and accurate long-range predictions of weather conditions are necessary to develop optimal agricultural strategies.

PDO is the dominant mode of the North Pacific. It has been described as the leading empirical orthogonal function of North Pacific sea surface temperature (SST) anomalies (Trenberth, 1990, 1994; Mantua et al., 1997). There are two phases of PDO. A positive phase occurs when the Aleutian low is deeper and negative SST anomalies occur in the north central Pacific; the negative phase is the opposite (Mantua et al., 1997). PDO appears to undergo rapid transitions between extended periods of the opposite phase every few decades or so (Mantua et al., 1997; Minobe, 1997; 1999). It has a profound influence on various components of the climate (Newman et al., 2016): PDO affects decadal climate variations over East and South Asia (Yu et al., 2015; Fan and Fan, 2017); PDO also drives North American droughts (Zhao et al., 2017; McCabe et al., 2012) and Australian rainfall anomalies (Sun et al., 2015; Arblaster et al., 2002), and, most recently, the climate warming hiatus (Kosaka et al., 2013). Crop production and available water resources are also influenced by PDO (Mantua et al., 1997; Miller et al., 2004). The effects of PDO on the Chinese climate have been well documented (Ma and Fu, 2006; Qian and Zhou, 2014;

Li et al., 2010; Zhou et al., 2013; Ma, 2007; Ding et al., 2014). For example, a warm PDO phase can result in above-normal precipitation over South China and continuing drought over North China (Ma, 2007; Zhou et al., 2013; Yang et al., 2017). Huang et al. (2020) suggested that the future projections of the South Asian summer monsoon (SASM) also depend on the PDO phase transition, because the positive phases of PDO often lead to decreased SASM rainfall (Krishnamurthy and Krishnamurthy, 2014). In the positive phase, the winter temperature increases in China (Ding et al., 2014; Xu et al., 2019). Recent studies in many countries have investigated relationships between PDO teleconnections and crop yields. For example, in the southeastern United States, winter crop production is strongly correlated with decadal climate indices, and the negative PDO phase is associated with a low wheat yield (Tian, 2015). There is a pronounced increase in corn and soybean yields in Missouri when El Niño and a positive PDO phase occur together (Henson, 2017). However, similar studies that relate PDO cycles to crop production are not extensive in China, and the links are inconclusive. Huang et al. (2017) investigated the atmospheric circulation underlying changes in rice production in Jiangsu province due to meteorological disasters and found that PDO significantly influenced those changes. Liu et al. (2017) examined the impact of floods on agriculture in the Poyang Lake basin and investigated relationships with climate indices and found that PDO had no significant influence. PDO is a major factor in decadal climate prediction (Qin et al., 2018), therefore the possibility of nexus between PDO and other meteorological factors provides an opportunity to observe and understand the effects of climate patterns on crop production.

China is the world's largest wheat producer and provides about one-fifth of the global total. Even a small change in yields could have large global effects (Dawe, 2009; Simelton, 2011). Crop production is susceptible to variations in climate (Simelton, 2011). Climate variability in China is dominated by the East Asian monsoon (EAM) (Chen et al., 2019; Wang and Chen, 2014; Ding and Chan, 2005), which is significantly influenced by PDO (Wang et al., 2007, 2008a). However, owing to the long period ranges of PDO and the scarcity of statistical yield data in China, given the complexities involved in this

Accepted Article

issue, the impacts of PDO on winter wheat yields in China and the possible mechanism underlying the impact remain little understood (Tian et al., 2015; Fan and Fan, 2017; Huang et al., 2020).

To fill this knowledge gap, over one hundred years of winter wheat yields were simulated by utilizing a dynamic process crop growth model over eight representative locations in the dominant winter wheat-producing provinces across China. Since variability in crop yields is driven by numerous factors apart from climate fluctuations and agronomic management, such as sow data, cultivar choice and plant density (Tian et al., 2015), in this study, the DSSAT 4.7 CERES-wheat model was used to analyze the response of winter wheat yields to PDO by keeping all other factors constant over time. The completely observed weather data over multiple decades are difficult to obtain, so reanalysis data were used as a surrogate for inputs into the crop model in this study (Cammarano et al., 2013; Tian et al., 2015). The main goals of this study were to use wavelet transforms and ensemble empirical mode decomposition (EEMD) filters to investigate interdecadal climate variations and the drivers associated with PDO for effects on winter wheat yields in China. Then, we identified mechanisms by which different phases of PDO affected winter wheat yields. The outcomes of the study will provide a useful reference for predicting crop yields.

2 Materials and methods

2.1 Data

The major winter wheat growing regions are located in east-central parts of China, including Shandong, Henan, Hebei, Jiangsu, Hubei, Shanxi, Shaanxi and Anhui provinces (Song et al., 2019). In this study, we selected eight representative locations that (1) were located in the main producing areas of winter wheat, (2) were geographically different, (3) had good records of crop data for 1950–2014 (Figure 1). Historical annual winter wheat yield data (in kg/ha) from 1950 to 2014 were provided by the National Bureau of Statistics (<http://data.stats.gov.cn/index.htm>), which were used as a basis for comparison with the simulation results. Crop yields can be increased with advanced agricultural

techniques and additional production inputs; winter wheat yields were linearly detrended and adjusted to a 2000 baseline using a linear trend analysis technique to eliminate the effects of these activities (Swanson and Nyankori, 1979; Hollinger and Carlson, 2001; Xiong et al., 2008).

Monthly data on precipitation, maximum temperature, minimum temperature and number of wet days for $0.5^{\circ} \times 0.5^{\circ}$ grid resolution grids from 1902 to 2014 were obtained from the Climatic Research Unit (CRU TS 4.04) (<http://www.cru.uea.ac.uk/data>). Monthly maximum temperature and minimum temperature were interpolated to daily values by using spline interpolation (Vetterling and Press, 1992; Tao et al., 2009). Monthly precipitation is interpolated to daily values using a weather generator with total monthly precipitation and wet days as inputs. The occurrence of daily rainfall is described by a Markov chain and then a gamma distribution function is applied to fit the amount of rainfall on a rainy day (Geng et al., 1986). Studies have shown that simulations using interpolated and observed daily data are nearly identical (Tao et al., 2009; Gerten et al., 2004; Shuai et al., 2016). Daily solar radiation for each grid were obtained from NOAA-CIRES 20th Century Reanalysis V2c (https://www.psl.noaa.gov/data/gridded/data.20thC_ReanV2c.html). PDO time series data from 1902 to 2014 were obtained from the Joint Institute for the Study of the Atmosphere and Ocean (JISAO) by downloading from <http://research.jisao.washington.edu/pdo/>.

2.2 Crop simulation

Crop simulation was performed using the DSSAT 4.7 CERES-wheat model. Input requirements for CERES-wheat include weather and soil conditions, plant characteristics and crop management (Hunt et al., 2001). The Generalized Likelihood Uncertainty Estimation (GLUE) program of DSSAT was used to estimate the cultivar coefficients of the winter wheat. The coefficients of a representative cultivar were estimated iteratively by running the model with an altered coefficient and comparing the simulated outputs with observed values until they matched as closely as possible. For this study, the model

was calibrated and validated using trial data from eight representative locations for winter wheat (from 2005 to 2014). Figure 2 shows the relationship between the observed and simulated values of yields; the root mean square error (RMSE) between the observed and estimated yields was 18.17%, and the estimated values agreed well with the observed values. The calibrated cultivars are shown in Table 1.

Soil Characteristics were specified for crop model simulations at each site based on Jin et al. (1995). The agricultural soils of the main producing area of winter wheat are primarily sandy-loam of medium depth, with neutral pH and low-to moderate level of organic carbon (Rosenzweig et al., 1999). The wheat model was simulated with a rained (non-irrigated) scheme and with no nitrogen (N) stress. The planting density was 200 plants m⁻². Winter wheat in China is usually sown in October or November and harvested in the following May and June. The planting dates were chosen as average planting dates for these eight locations (Table 1) according to Zhuang et al. (2018). The soil water content was initialized in the model before the sowing date to avoid any variability in water carry-over effects.

2.3 Wavelet method

The wavelet method is based on the assumption that climate variation patterns result from nonstationary processes in which variance, frequency, and oscillation duration vary over time (Grinsted et al., 2004). Recently, wavelet transforms have been used in correlation analysis between nonstationary time series in different fields, such as climatology and hydrology (Liang et al., 2010; Rahman and Islam, 2019). Earlier studies that have shown relationships between crop yield and teleconnection indices implicitly assumed that time series represent stationary processes and so used correlation- or regression-based models. The continuous wavelet transform (CWT) is a commonly used technique to detect localized variation in a time series. The cross wavelet transform (XWT) is a powerful method of testing for relationships between two time series. A detailed discussion of CWT and XWT is given in Torrence and Compo (1998).

The CWT of a discrete sequence X_n is defined as the convolution of X_n with a scaled and translated version of $\Psi_0(\eta)$:

$$W_n(s) = \sum_{n=0}^{N-1} \chi_n \psi^* \left[\frac{(n'-n)\delta t}{s} \right] \quad (1)$$

where s is the wavelet scale, n is the localized time index, (*) indicates the complex conjugate, δt is the sampling interval, N is the number of points in the time series, and $|W_n(s)|^2$ is defined as the wavelet power spectrum, which expresses the amplitude of the time series in a given wavelet scale (Lafrenière and Sharp, 2003). The mother wavelet is $\Psi_0(\eta)$; the Morlet wavelet, which consists of a plane wave modulated by a Gaussian window, was used in this study:

$$\psi_0(\eta) = \pi^{-1/4} e^{i\omega_0\eta} e^{-\eta^2/2} \quad (2)$$

where ω_0 is dimensionless frequency, and η is dimensionless time. By averaging the wavelet power spectrum over the period, we obtain the global wavelet spectrum:

$$\bar{W}^2(s) = \frac{1}{N} \sum_{n=0}^{N-1} |W_n(s)|^2 \quad (3)$$

For two time series X and Y , with wavelet transforms $W_n^X(s)$ and $W_n^Y(s)$, the cross wavelet spectrum of X and Y is defined as $W_n^{XY}(s) = W_n^X(s)W_n^{Y*}(s)$, where $W_n^{Y*}(s)$ is the complex conjugate of $W_n^Y(s)$. The cross wavelet transform is defined as $|W_n^{XY}(s)|$.

The cone of influence (COI) is that region of the wavelet spectrum in which edge effects become important. It is chosen so that a discontinuity at the edge drops by a factor e^{-2} to ensure that edge effects are negligible before this point. The 95% confidence level of the power spectrums was assessed against the null hypothesis that the time series was generated as red noise (Torrence and Compo, 1998).

2.4 Ensemble empirical mode decomposition

To detect the relationship between PDO and winter wheat yield on interdecadal scales, the EEMD method was used. EEMD is a pre-processing data-adaptive filter for time series datasets that increases the robustness of noisy data and guarantees that the

Accepted Article

decomposition is insensitive to noise. EEMD is suitable for analyzing meteorological data, which are usually nonstationary and nonlinear, and contain noise (Huang and Wu, 2008; Wu and Huang, 2009; Liu and Zhou et al., 2019). It has been used to distinguish the interdecadal variations in temperature, precipitation, drought index, etc., and the results shows clear physical significance (Qian and Zhou, 2014; Yang et al., 2017). In this study, EEMD was used to extract interdecadal variation components from the PDO, winter wheat yield and climate factors (mean temperature and precipitation) from 1902 to 2014. EEMD was also used to determine the timings of the phase transitions in the PDO index; data for the years analyzed in the study were divided into three negative phases (1906–1924, 1945–1975 and 2003–2014) and two positive phases (1925–1944 and 1976–2002).

The contribution rate of PDO to winter wheat yields (q) is quantified by:

$$q = \left| \frac{Y_w - Y_c}{Y} \right| \times 100\% \quad (4)$$

where Y_w and Y_c are the averages of winter wheat yields during the warm and cold phases of PDO, respectively. Y is the average of raw winter wheat yield.

3 Results

3.1 Variability of winter wheat yields

The continuous wavelet transform (CWT) of annual winter wheat production for each site is shown in Figure 3. Winter wheat yield was dominated by the decadal variability with a 22-year period in eight representative locations, and there were shorter 4-year and 8-year periods of variability in most wheat-growing sites. The wavelet power spectrums of winter wheat yields were high from the 1920s to the 1940s, with a 4-year period in Nanjing, Wuhan and Shijiazhuang. Winter wheat yield showed an inter-annual variability with an 8-year period in Nanjing, Hefei, Shijiazhuang, Wuhan, Zhengzhou and Xi'an from the 1920s to the 1950s, and there was an 8-year period in Jinan, Zhengzhou, Xi'an and Taiyuan from the 1980s to the 1990s. The wavelet power spectrums of winter wheat yields were relatively high from the 1940s to the 1980s for a 22-year period. It

should be noted that the CWT has identified a longer oscillation (more than 50 years) in eight sites, which is above the 5% significance level, although most of the occurrence of decadal variations were outside the cone of influence (COI) because of the study period. These interdecadal variations were probably related to the periods of PDO, whose highest energetic periodic variations at the decadal scale is 15–25 and 50–70 years. However, winter wheat yields can be affected by various factors. It is difficult to tell if it is a coincidence, but the cross wavelet transform (XWT) will help in this regard.

3.2 Relationship between PDO and winter wheat yields

Figure 4 shows the XWT of winter wheat yields and PDO in China. The relative phase relationship is shown as arrows (with in-phase pointing right, anti-phase pointing left). The cross wavelet power spectrum was high for the 22-year oscillation in eight sites from the 1940s to the 1980s and the phase relationship was ‘in phase’. The cross wavelet power spectrum was high for a shorter 8-year period from the 1980s to the 1990s in Jinan, Xi’an, Zhengzhou and Taiyuan, which could be associated with a PDO-ENSO interaction (Henson et al., 2017). We also note that there is a significant common power over the 50 years in eight sites, which confirms the assumption of CWT in Figure 3. The XWT shows that the winter wheat yield and PDO are in phase in all sectors with a significant common power, which suggests that a positive (negative) PDO is associated with a high (low) winter wheat yield.

EEMD was used to identify interdecadal components to determine the interdecadal relationship between PDO and winter wheat yields. Table 2 shows the mean periods of various time-scale components for PDO, winter wheat yield, mean temperature and precipitation during 1902–2014 obtained by the EEMD method, respectively. PDO and winter wheat yields were decomposed into six partitions, C1–C5. C1 and C2 represent the inter-annual variability; C3, C4 and C5 represent variability from the decadal to interdecadal scales. We used the sum of C4 and C5, which represents the interdecadal variability of winter wheat yields and PDO. Figure 5 shows the normalized interdecadal time series for PDO and winter wheat yields for eight sites using the EEMD filter. PDO

and winter wheat yields show an evident corresponding variation on the interdecadal scale: when PDO is in a positive (negative) phase, winter wheat yields show positive (negative) anomalies, suggesting that when the PDO is in a positive (negative) phase, winter wheat yields tend to increase (decrease). This corresponds to the XWT results shown in Figure 4. In addition, the mean correlation coefficient between PDO and winter wheat yields was 0.83 (Figure 6), which is statistically significant at the 0.01 level by the Student's t -test. For data extracted using the EEMD method, the significance was determined by an effective degree of freedom of 58 when considering the autocorrelations. This effective degree of freedom is calculated as

$$N_{edof} = N \frac{1 - r_1 r_2}{1 + r_1 r_2} \quad (5)$$

where N is the original sample size of 1000, and r_1 (r_2) is the lag-1 autocorrelation of the first (second) time series (Bretherton et al., 1999). According to Eq. (4), the mean contribution rate of PDO to winter wheat yields was 11% for eight representative sites.

3.3 Possible mechanism for PDO on winter wheat yields

Climate factors, particularly temperature and precipitation, which are affected by PDO (Ding et al., 2014; Liu et al., 2019; Yang et al., 2017), have a significant influence on the interdecadal variation in crop production (Henson et al., 2017). To further analyze the mechanism behind the impacts of PDO on winter wheat yields, the interdecadal variation components from mean temperature and precipitation were extracted, similar to PDO and winter wheat yields before. It can guarantee that impacts of climate factors on winter wheat yields were contributed from PDO, excluding the effects of external factors with periods shorter than PDO (like ENSO) and longer than PDO (like AMO). We calculated correlation coefficients between winter wheat yields and monthly precipitation and temperature during the growing season on the interdecadal scale (Figure 6) to further examine the modulation of crop yields by PDO. Winter wheat yields for eight sites all have a strong negative correlation with April precipitation and a positive correlation with December temperature. The mean correlation coefficients between December

temperature and April precipitation for eight sites were 0.59 and -0.50 with an effective degree of freedom of 58 (>99% confidence level), respectively. The correlations indicated that interdecadal variations in winter wheat yields were mostly related to April precipitation and December temperature.

Since April precipitation and December temperature associated with PDO had a profound effect on winter wheat yields on the interdecadal scale, we therefore performed a composite analysis of PDO negative phases (1906–1924, 1945–1975 and 2003–2014) minus PDO positive phases (1925–1944 and 1976–2002) for mean April precipitation (Figure 7a) and December temperature (Figure 7b). There are positive (negative) April precipitation anomalies and negative (positive) December temperature anomalies over the winter wheat production areas during the negative (positive) phases of PDO. This feature of April precipitation was consistent with Yang et al. (2017). They extracted the interdecadal components of PDO and monthly precipitation over China and calculated the correlation coefficients between them, the results of which show that April precipitation exhibits a significant negative correlation with PDO. This is because there are high (low) pressure anomalies over North Pacific at 500 hPa in April during the positive (negative) phase of PDO and southeasterly winds over North China promote northward transport of moisture. Besides, this outcome was also supported by Qian and Zhou (2014), who analyzed the relationship between PDO and a drought severity index calculated from three datasets and reported that the positive PDO corresponds to a dry period in North China. During winter, the winter temperature is positively correlated with PDO. This correlation is consistent throughout China, and is particularly strong in North China, which is associated with deeper (weaker) East Asian trough, stronger (weaker) Siberian high and anomalous cyclone (anticyclone) at 850 hPa over the eastern Philippines during the negative (positive) phase of PDO (Ding et al., 2014).

4 Discussion

In this study, we detected short term (4-year and 8-year) and long term decadal (22-year and over 50-year) climate-driven variations in simulated winter wheat yields in

representative locations in the dominant winter wheat producing areas over China. The 4-year and 8-year periods could be associated with the influence of ENSO and ENSO-PDO, respectively (Henson et al., 2017). Although PDO varies greatly over cycles of 4 or 8 years to decades, its highest energetic periodic variation on the decadal scale is 15–25 and 50–70 years (Qian and Zhou, 2014). The XWT was used to determine if the resulting decadal oscillations related to the PDO variability. The XWT of the simulated winter wheat yields and PDO showed that there was a significant common power in the 22-year and 50-year periods. To further investigate the interdecadal relationship between PDO and winter wheat yields, we used the EEMD method to extract interdecadal variation components from PDO and winter wheat yields. PDO and winter wheat yields showed evident corresponding variations. The contribution rate of PDO to winter wheat yields was approximately 11%. The interdecadal variation of winter wheat yields was associated with interdecadal variations in December temperature and April precipitation, which were modulated by PDO. The mean correlation coefficients between December temperature and April precipitation for eight sites were 0.59 and -0.50, respectively, which is statistically significant at 0.01 level. This is because December temperature is important for winter wheat to tiller; during the tillering stage, a higher temperature could significantly promote tillering and increase the effective panicles, which increased grain yields compared with a lower temperature (Fang et al., 2012). Tillering is regarded as an expression of certain characteristics of the plant, which is associated or correlated with desirable qualities. The wheat plant responds to a favorable environment by increasing the number of culms rather than by lengthening it or by increasing the number of grains in the spike (Grantham, 1912). More importantly, an increase in the number of tillers per plant is accompanied by a higher yield per spike. At this point, during the negative phase of PDO, lower December temperatures limited tillering and reduced the effective panicles, indirectly causing reductions in winter wheat yields. In the meantime, the temperature decrease during winter may directly increase frost/chilling and indirectly increase heat injury due to warming-led earlier anthesis (Porter et al., 1999; Sadras and Monzon, 2006; Wang et al., 2008b). Figure 7(b) suggests that during the negative

(positive) phase of PDO, there was a lower December temperature in the winter wheat producing area. The interdecadal variations in yields were related to interdecadal oscillations in April precipitation because April precipitation determines soil water availability to wheat crops during stem elongation, heading, and flowering stages. Figure 7(a) suggests that during the negative (positive) period of PDO, there was more (less) precipitation in the producing area. Excess rainfall is associated with flood, plant diseases, and insect pest outbreaks that adversely affect winter wheat production and its quality (Wiik and Ewaldz, 2009). During April, winter wheat is in the heading stage (Zhuang et al., 2018). Increased precipitation during this stage can result in diseases such as *fusarium* head blight (FHB), *Puccinia striiformis* growth and sheath blight, which reduce both the quantity and quality of the crop (Song et al., 2019). Thus, there is a need for governments and farmers to recognize the hazards of excess April precipitation and low December temperature in negative PDO years.

These outcomes are important because insights into the association between decadal climate variability and local seasonal climate variability are useful for further seasonal predictions that enable growers to increase seasonal agricultural crop growth. For example, knowledge and understanding of the positive and negative phases of PDO increase our understanding of the effects of large-scale atmospheric circulation on winter wheat yields. The effects of PDO climate patterns are not limited to a specific region, and crop production, water resources and other agricultural inputs are also affected by PDO (Miller et al., 2004). The winter wheat yield increases during positive PDO years and decreases in negative PDO years in the representative sites, but these PDO-influenced climate patterns are important for winter wheat production in other regions of the world (Atkinson et al., 2005; Persson et al., 2012; Tian et al., 2015; Newman et al., 2016). Such knowledge is useful as a reference for strategic decision-making in adapting to climate events for the benefit of crop growers. The long term climate patterns of PDO can now be incorporated when considering climate effects on regional agricultural crop production, similar to how we consider them on a regional scale (Izumi et al., 2014).

This paper provides a preliminary analysis of the relationship between PDO and winter wheat yields. Further research will provide a more precise description of PDO–crop growth mechanisms. The impact of extreme events was not considered in this study, nor were technological development or changes in agricultural practice. Climate change and associated extreme events are an increasing concern, and the relationship between extreme climate events and crop growth must be emphasized in future research.

5 Conclusion

In this study, we simulated winter wheat yields for 1902–2014 using the DSSAT 4.7 CERES-wheat model. The relationship between PDO and winter wheat yields in eight representative sites over major winter wheat-producing regions of China was investigated using the cross wavelet transform (XWT) analysis and EEMD filter. The main findings are summarized as follows:

- (1) Winter wheat yields in China were investigated to identify periodicities by CWT. We found a short term (4-year and 8-year periods) and long term variation (22-year and over 50-year periods).
- (2) PDO and winter wheat yields show an evident corresponding variation on the interdecadal scale: when PDO is in a positive (negative) phase, winter wheat yields shows positive (negative) anomalies, suggesting that when PDO is in a positive (negative) phase, winter wheat yields tend to increase (decrease). This agrees with the outcomes of XWT.
- (3) By using the EEMD method, the interdecadal variation components from winter wheat yields and PDO were extracted. The winter wheat yields were significantly positively correlated with the PDO index on the interdecadal scale and the mean correlation coefficient was 0.83. The mean contribution rate of PDO to winter wheat yields was 11% for eight representative sites, which quantified the impact of PDO on winter wheat yields.
- (4) The interdecadal variation of winter wheat yields was associated with interdecadal variations in December temperature and April precipitation, which were associated

with PDO. The mean correlation coefficients between winter wheat yields and December temperature and April precipitation for eight sites were 0.59 and -0.50, respectively, which are statistically significant at the 0.01 level.

- (5) April precipitation and December temperature anomalies are modulated by PDO: when PDO is in the negative (positive) phase, more (less) April precipitation and lower (higher) December temperature would occur in the study area. Similarly, increases (decreases) in April precipitation and a lower (higher) December temperature adversely (favorably) affect winter wheat in the heading and tillering stages, respectively, which will reduce both the quantity and quality of winter wheat. This clearly explains the impact of PDO on winter wheat yields in China. The obtained findings can aid policymakers and farmers in mitigating the adverse effect of winter wheat production losses in China.

Reference:

- ARBLASTER, J., MEEHL, G. & MOORE, A. 2002. Interdecadal modulation of Australian rainfall. *Climate Dynamics*, 18, 519-531.
- ATKINSON, M., KETTLEWELL, P., HOLLINS, P., STEPHENSON, D. & HARDWICK, N. 2005. Summer climate mediates UK wheat quality response to winter North Atlantic Oscillation. *Agricultural and Forest Meteorology*, 130, 27-37.
- BAIGORRIA, G. A., JONES, J. W. & O'BRIEN, J. J. 2008. Potential predictability of crop yield using an ensemble climate forecast by a regional circulation model. *Agricultural and Forest Meteorology*, 148, 1353-1361.
- BANNAYAN, M., SANJANI, S., ALIZADEH, A., LOTFABADI, S. S. & MOHAMADIAN, A. 2010. Association between climate indices, aridity index, and rainfed crop yield in northeast of Iran. *Field crops research*, 118, 105-114.
- BRETHERTON, C. S., WIDMANN, M., DYMNIKOV, V. P., WALLACE, J. M. & BLADÉ, I. 1999. The effective number of spatial degrees of freedom of a time-varying field. *Journal of climate*, 12, 1990-2009.
- BROWN, I. 2013. Influence of seasonal weather and climate variability on crop yields in Scotland. *International journal of biometeorology*, 57, 605-614.
- CAMMARANO, D., STEFANOVA, L., ORTIZ, B. V., RAMIREZ-RODRIGUES, M., ASSENG, S., MISRA, V., WILKERSON, G., BASSO, B., JONES, J. W. & BOOTE, K. J. 2013. Evaluating the fidelity of downscaled climate data on simulated wheat and maize production in the southeastern US. *Regional Environmental Change*, 13, 101-110.
- CHEN, W., WANG, L., FENG, J., WEN, Z., MA, T., YANG, X. & WANG, C. 2019. Recent progress in studies of the variabilities and mechanisms of the East Asian monsoon in a changing climate.

Advances in Atmospheric Sciences, 36, 887-901.

- DAWE, D. 2009. The unimportance of " low " world grain stocks for recent world price increases, Citeseer.
- DING, Y., LIU, Y., LIANG, S., MA, X., ZHANG, Y., SI, D., LIANG, P., SONG, Y. & ZHANG, J. 2014. Interdecadal variability of the East Asian winter monsoon and its possible links to global climate change. *Journal of Meteorological Research*, 28, 693-713.
- DING, Y. & CHAN, J. C. 2005. The East Asian summer monsoon: an overview. *Meteorology and Atmospheric Physics*, 89, 117-142.
- FAN, Y. & FAN, K. 2017. Pacific decadal oscillation and the decadal change in the intensity of the interannual variability of the South China Sea summer monsoon. *Atmospheric and Oceanic Science Letters*, 10, 162-167.
- FANG, S., TAN, K., REN, S., ZHANG, X. & ZHAO, J. 2012. Fields experiments in North China show no decrease in winter wheat yields with night temperature increased by 2.0–2.5 C. *Science China Earth Sciences*, 55, 1021-1027.
- GENG, S., DE VRIES, F. W. P. & SUPIT, I. 1986. A simple method for generating daily rainfall data. *Agricultural and Forest Meteorology*, 36, 363-376.
- GERTEN, D., SCHAPHOFF, S., HABERLANDT, U., LUCHT, W. & SITCH, S. 2004. Terrestrial vegetation and water balance—hydrological evaluation of a dynamic global vegetation model. *Journal of Hydrology*, 286, 249-270.
- GRANTHAM, A. 1912. Tillering as a Factor in Determining the Desirable Qualities of Winter Wheats. *Agronomy Journal*, 4, 75-81.
- GRINSTED, A., MOORE, J. C. & JEVREJEVA, S. 2004. Application of the cross wavelet transform and wavelet coherence to geophysical time series.
- HENSON, C., MARKET, P., LUPO, A. & GUINAN, P. 2017. ENSO and PDO-related climate variability impacts on Midwestern United States crop yields. *International journal of biometeorology*, 61, 857-867.
- HOLLINGER, S. E., EHLER, E. J. & CARLSON, R. E. 2001. Midwestern United States Corn and Soybean Yield Response to Changing El Niño-Southern Oscillation Conditions During the Growing Season. *Impacts of El Niño and climate variability on agriculture*, 63, 31-54.
- HOOGENBOOM, G. 2000. Contribution of agrometeorology to the simulation of crop production and its applications. *Agricultural and forest meteorology*, 103, 137-157.
- HUANG, J., LEI, Y., ZHANG, F. & HU, Z. 2017. Spatio-temporal analysis of meteorological disasters affecting rice, using multi-indices, in Jiangsu province, Southeast China. *Food Security*, 9, 661-672.
- HUANG, N. E. & WU, Z. 2008. A review on Hilbert-Huang transform: Method and its applications to geophysical studies. *Reviews of geophysics*, 46.
- HUANG, X., ZHOU, T., DAI, A., LI, H., LI, C., CHEN, X., LU, J. & WU, B. 2020. South Asian summer monsoon projections constrained by the interdecadal Pacific oscillation. *Science advances*, 6, eaay6546.
- HUNT, L., WHITE, J. & HOOGENBOOM, G. 2001. Agronomic data: advances in documentation and protocols for exchange and use. *Agricultural Systems*, 70, 477-492.
- IIZUMI, T., LUO, J.-J., CHALLINOR, A. J., SAKURAI, G., YOKOZAWA, M., SAKUMA, H., BROWN, M. E. & YAMAGATA, T. 2014. Impacts of El Niño Southern Oscillation on the global

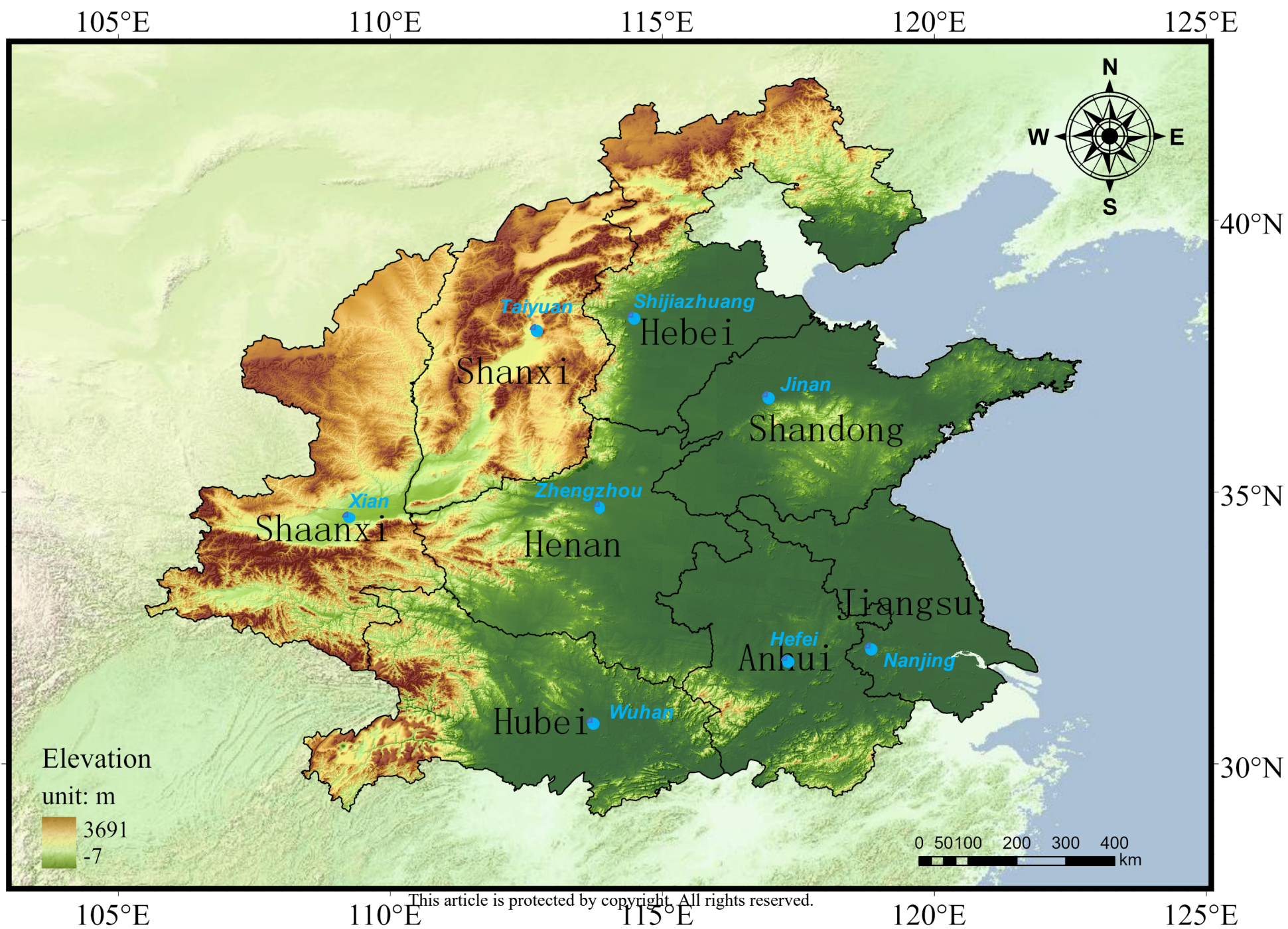
yields of major crops. *Nature communications*, 5, 1-7.

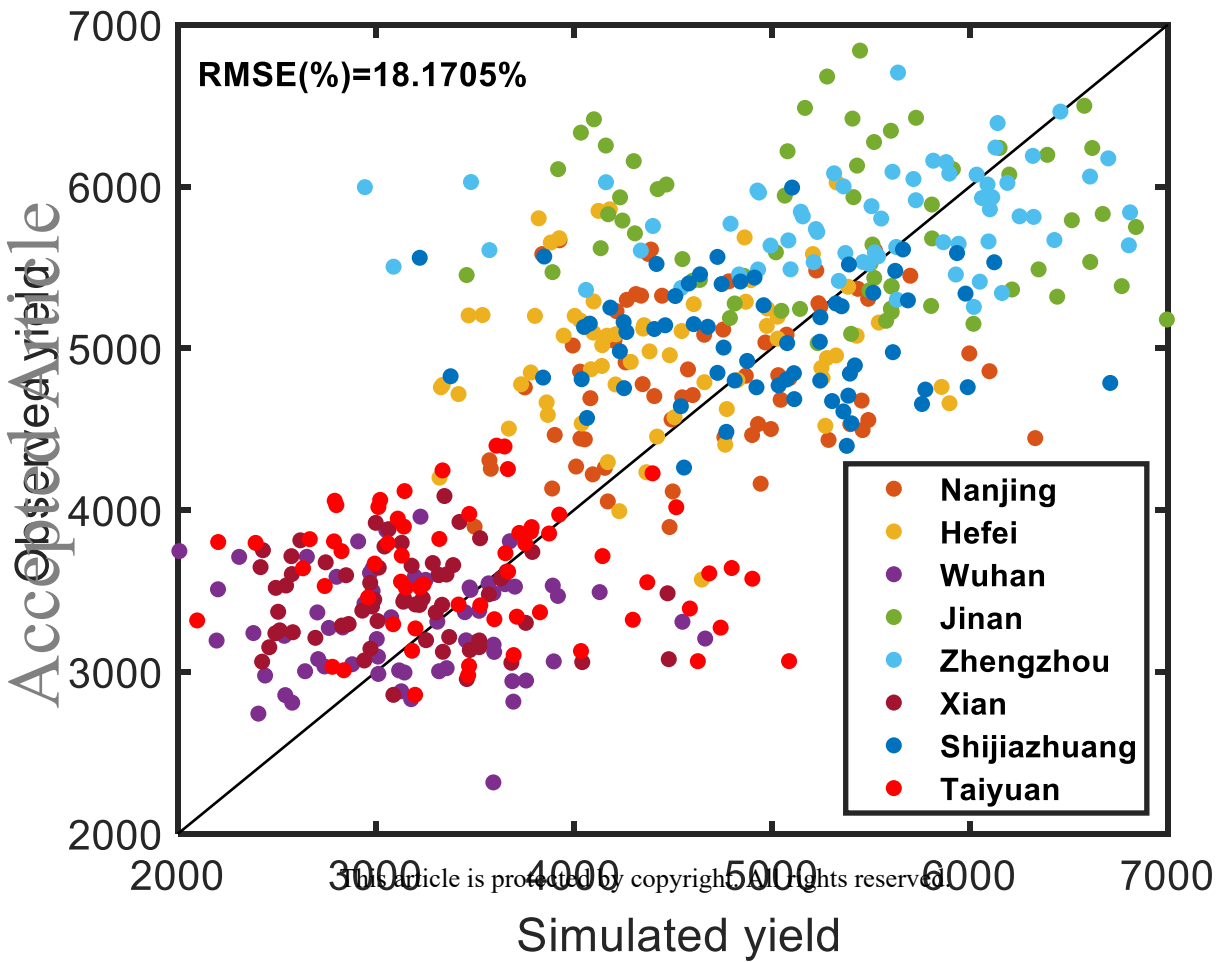
- JARLAN, L., ABAOUI, J., DUCHEMIN, B., OULDBBA, A., TOURRE, Y., KHABBA, S., LE PAGE, M., BALAGHI, R., MOKSSIT, A. & CHEHBOUNI, G. 2014. Linkages between common wheat yields and climate in Morocco (1982–2008). *International journal of biometeorology*, 58, 1489-1502.
- JIN, Z., GE, D., CHEN, H. & FANG, J. 1995. Effects of climate change on rice production and strategies for adaptation in southern China. *Climate change and agriculture: Analysis of potential international impacts*, 59, 307-323.
- KOSAKA, Y. & XIE, S.-P. 2013. Recent global-warming hiatus tied to equatorial Pacific surface cooling. *Nature*, 501, 403-407.
- KRISHNAMURTHY, L. & KRISHNAMURTHY, V. 2014. Influence of PDO on South Asian summer monsoon and monsoon–ENSO relation. *Climate Dynamics*, 42, 2397-2410.
- LAFRENIERE, M. & SHARP, M. 2003. Wavelet analysis of inter-annual variability in the runoff regimes of glacial and nival stream catchments, Bow Lake, Alberta. *Hydrological Processes*, 17, 1093-1118.
- LI, H., DAI, A., ZHOU, T. & LU, J. 2010. Responses of East Asian summer monsoon to historical SST and atmospheric forcing during 1950–2000. *Climate Dynamics*, 34, 501-514.
- LI, Y., STRAPASSON, A. & ROJAS, O. 2020. Assessment of El Niño and La Niña impacts on China: Enhancing the Early Warning System on Food and Agriculture. *Weather and Climate Extremes*, 27, 100208.
- LIANG, S., GE, S., WAN, L. & ZHANG, J. 2010. Can climate change cause the Yellow River to dry up? *Water Resources Research*, 46.
- LIU, J., ZHANG, Q., SINGH, V. P., GU, X. & SHI, P. 2017. Nonstationarity and clustering of flood characteristics and relations with the climate indices in the Poyang Lake basin, China. *Hydrological Sciences Journal*, 62, 1809-1824.
- LIU, Q., ZHOU, T., MAO, H. & FU, C. 2019. Decadal variations in the relationship between the western Pacific subtropical high and summer heat waves in East China. *Journal of Climate*, 32, 1627-1640.
- MA, Z. 2007. The interdecadal trend and shift of dry/wet over the central part of North China and their relationship to the Pacific Decadal Oscillation (PDO). *Chinese Science Bulletin*, 52, 2130-2139.
- MA, Z. & FU, C. 2006. Some evidence of drying trend over northern China from 1951 to 2004. *Chinese Science Bulletin*, 51, 2913-2925.
- MANTUA, N. J., HARE, S. R., ZHANG, Y., WALLACE, J. M. & FRANCIS, R. C. 1997. A Pacific interdecadal climate oscillation with impacts on salmon production. *Bulletin of the American Meteorological Society*, 78, 1069-1080.
- MAXWELL, J. T., KNAPP, P. A. & ORTEGREN, J. T. 2013. Influence of the Atlantic Multidecadal Oscillation on tupelo honey production from AD 1800 to 2010. *Agricultural and forest meteorology*, 174, 129-134.
- MCCABE, G. J., AULT, T. R., COOK, B. I., BETANCOURT, J. L. & SCHWARTZ, M. D. 2012. Influences of the El Niño Southern Oscillation and the Pacific Decadal Oscillation on the timing of the North American spring. *International Journal of Climatology*, 32, 2301-2310.
- MILLER, A. J., CHAI, F., CHIBA, S., MOISAN, J. R. & NEILSON, D. J. 2004. Decadal-scale climate and ecosystem interactions in the North Pacific Ocean. *Journal of Oceanography*, 60, 163-188.
- MINOBE, S. 1997. A 50–70 year climatic oscillation over the North Pacific and North America.

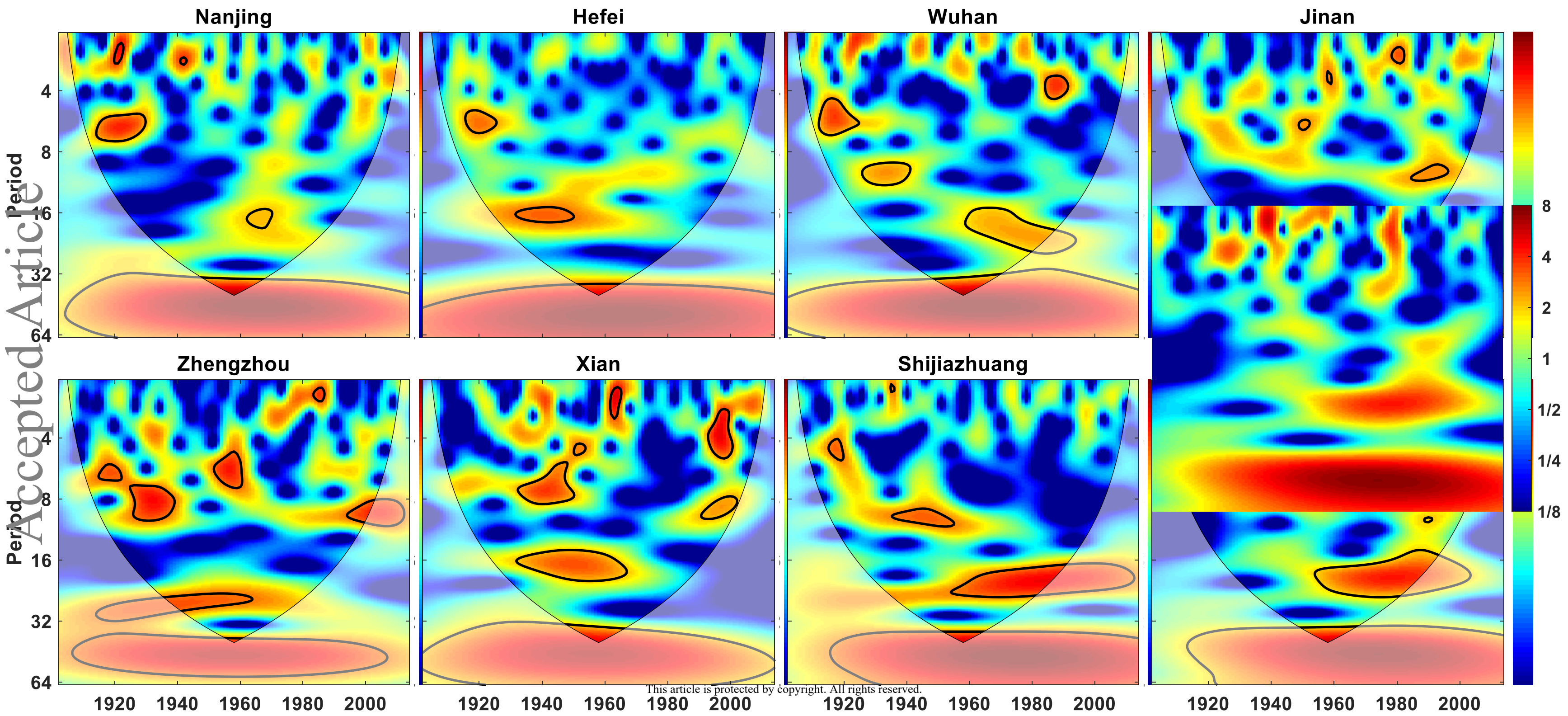
- Geophysical Research Letters, 24, 683-686.
- MINOBE, S. 1999. Resonance in bidecadal and pentadecadal climate oscillations over the North Pacific: Role in climatic regime shifts. *Geophysical Research Letters*, 26, 855-858.
- NEWMAN, M., ALEXANDER, M. A., AULT, T. R., COBB, K. M., DESER, C., DI LORENZO, E., MANTUA, N. J., MILLER, A. J., MINOBE, S. & NAKAMURA, H. 2016. The Pacific decadal oscillation, revisited. *Journal of Climate*, 29, 4399-4427.
- NICHOLLS, N. 1997. Increased Australian wheat yield due to recent climate trends. *Nature*, 387, 484-485.
- PERSSON, T., BERGJORD, A. K. & HÖGLIND, M. 2012. Simulating the effect of the North Atlantic Oscillation on frost injury in winter wheat. *Climate Research*, 53, 43-53.
- PORTER, J. R. & GAWITH, M. 1999. Temperatures and the growth and development of wheat: a review. *European journal of agronomy*, 10, 23-36.
- QIAN, C. & ZHOU, T. 2014. Multidecadal variability of North China aridity and its relationship to PDO during 1900–2010. *Journal of Climate*, 27, 1210-1222.
- QIN, M., LI, D., DAI, A., HUA, W. & MA, H. 2018. The influence of the Pacific Decadal Oscillation on North Central China precipitation during boreal autumn. *International Journal of Climatology*, 38, e821-e831.
- RAHMAN, M. S. & ISLAM, A. R. M. T. 2019. Are precipitation concentration and intensity changing in Bangladesh overtimes? Analysis of the possible causes of changes in precipitation systems. *Science of The Total Environment*, 690, 370-387.
- REN, S., QIN, Q. & REN, H. 2019. Contrasting wheat phenological responses to climate change in global scale. *Science of The Total Environment*, 665, 620-631.
- ROSENZWEIG, C., IGLESIAS, A., FISCHER, G., LIU, Y., BAETHGEN, W. & JONES, J. W. 1999. Wheat yield functions for analysis of land-use change in China. *Environmental Modeling & Assessment*, 4, 115-132.
- ROSENZWEIG, C., IGLESIUS, A., YANG, X.-B., EPSTEIN, P. R. & CHIVIAN, E. 2001. Climate change and extreme weather events-Implications for food production, plant diseases, and pests.
- SADRAS, V. O. & MONZON, J. P. 2006. Modelled wheat phenology captures rising temperature trends: Shortened time to flowering and maturity in Australia and Argentina. *Field crops research*, 99, 136-146.
- SHUAI, J., ZHANG, Z., SUN, D.-Z., TAO, F. & SHI, P. 2013. ENSO, climate variability and crop yields in China. *Climate research*, 58, 133-148.
- SHUAI, J., ZHANG, Z., TAO, F. & SHI, P. 2016. How ENSO affects maize yields in China: understanding the impact mechanisms using a process-based crop model. *International Journal of Climatology*, 36, 424-438.
- SIMELTON, E. 2011. Food self-sufficiency and natural hazards in China. *Food Security*, 3, 35-52.
- SONG, Y., LINDERHOLM, H. W., WANG, C., TIAN, J., HUO, Z., GAO, P., SONG, Y. & GUO, A. 2019. The influence of excess precipitation on winter wheat under climate change in China from 1961 to 2017. *Science of The Total Environment*, 690, 189-196.
- SUN, C., LI, J., FENG, J. & XIE, F. 2015. A decadal-scale teleconnection between the North Atlantic Oscillation and subtropical eastern Australian rainfall. *Journal of Climate*, 28, 1074-1092.
- SWANSON, E. R. & NYANKORI, J. C. 1979. Influence of weather and technology on corn and soybean yield trends. *Agricultural Meteorology*, 20, 327-342.

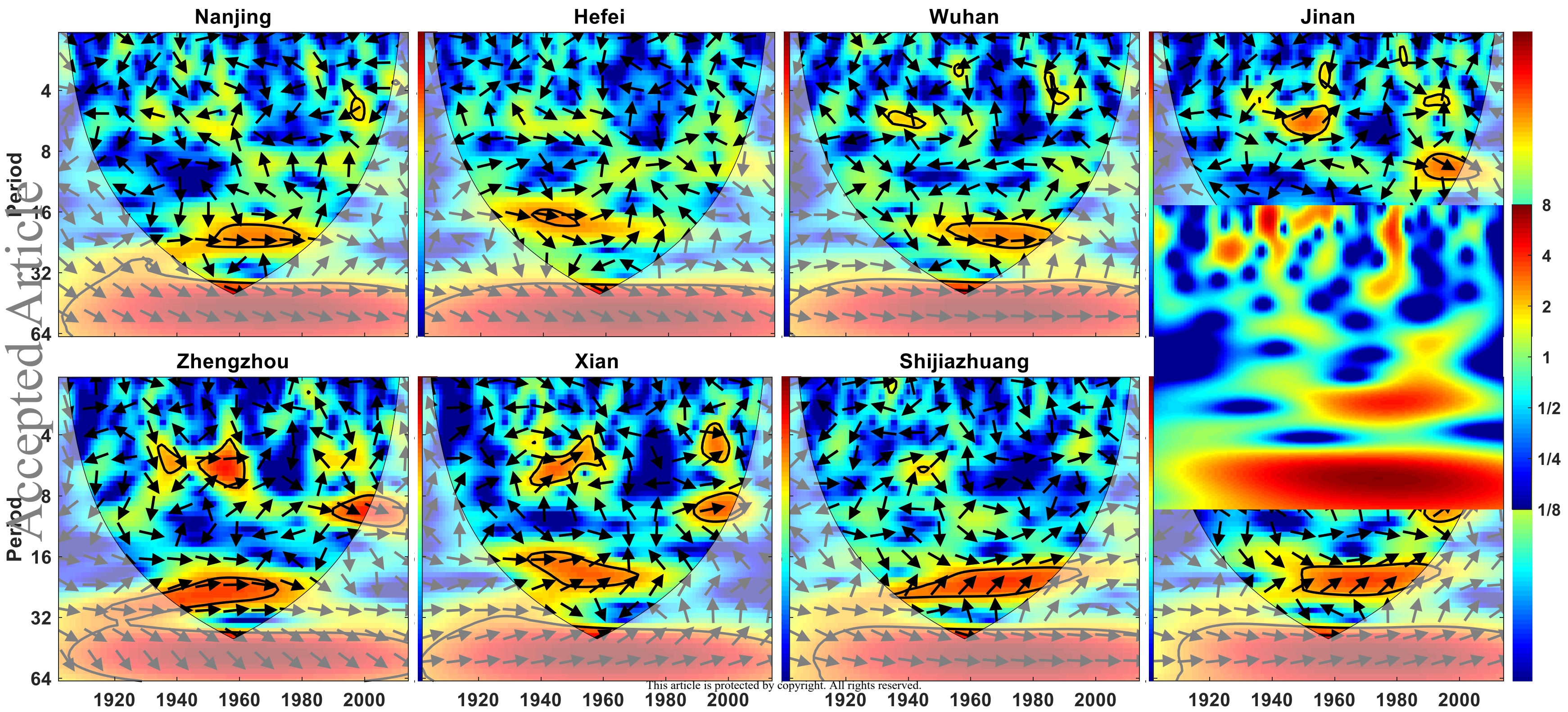
- TAO, F., YOKOZAWA, M. & ZHANG, Z. 2009. Modelling the impacts of weather and climate variability on crop productivity over a large area: a new process-based model development, optimization, and uncertainties analysis. *Agricultural and forest meteorology*, 149, 831-850.
- TIAN, D., ASSENG, S., MARTINEZ, C. J., MISRA, V., CAMMARANO, D. & ORTIZ, B. V. 2015. Does decadal climate variation influence wheat and maize production in the southeast USA? *Agricultural and forest meteorology*, 204, 1-9.
- TORRENCE, C. & COMPO, G. P. 1998. A practical guide to wavelet analysis. *Bulletin of the American Meteorological society*, 79, 61-78.
- TRENBERTH, K. E. 1990. Recent observed interdecadal climate changes in the Northern Hemisphere. *Bulletin of the American Meteorological Society*, 71, 988-993.
- TRENBERTH, K. E. & HURRELL, J. W. 1994. Decadal atmosphere-ocean variations in the Pacific. *Climate Dynamics*, 9, 303-319.
- VETTERLING, W. T. & PRESS, W. H. 1992. Numerical recipes in Fortran: the art of scientific computing, Cambridge University Press.
- WANG, L., CHEN, W. & HUANG, R. 2008a. Interdecadal modulation of PDO on the impact of ENSO on the East Asian winter monsoon. *Geophysical Research Letters*, 35.
- WANG, H., GAN, Y., WANG, R., NIU, J., ZHAO, H., YANG, Q. & LI, G. 2008b. Phenological trends in winter wheat and spring cotton in response to climate changes in northwest China. *Agricultural and Forest Meteorology*, 148, 1242-1251.
- WANG, L. & CHEN, W. 2014. An intensity index for the East Asian winter monsoon. *Journal of Climate*, 27, 2361-2374.
- WANG, L., CHEN, W. & HUANG, R. 2007. Changes in the variability of North Pacific Oscillation around 1975/1976 and its relationship with East Asian winter climate. *Journal of Geophysical Research: Atmospheres*, 112.
- WIJK, L. & EWALDZ, T. 2009. Impact of temperature and precipitation on yield and plant diseases of winter wheat in southern Sweden 1983–2007. *Crop Protection*, 28, 952-962.
- WU, Z. & HUANG, N. E. 2009. Ensemble empirical mode decomposition: a noise-assisted data analysis method. *Advances in adaptive data analysis*, 1, 1-41.
- XIONG, W., CONWAY, D., HOLMAN, I. & LIN, E. 2008. Evaluation of CERES-Wheat simulation of Wheat Production in China. *Agronomy Journal*, 100, 1720-1728.
- XU, Y., LI, T., SHEN, S. & HU, Z. 2019. Assessment of CMIP5 Models Based on the Interdecadal Relationship between the PDO and Winter Temperature in China. *Atmosphere*, 10, 597.
- YANG, Q., MA, Z. & XU, B. 2017. Modulation of monthly precipitation patterns over East China by the Pacific Decadal Oscillation. *Climatic change*, 144, 405-417.
- YU, L., FUREVIK, T., OTTERÅ, O. H. & GAO, Y. 2015. Modulation of the Pacific Decadal Oscillation on the summer precipitation over East China: a comparison of observations to 600-years control run of Bergen Climate Model. *Climate Dynamics*, 44, 475-494.
- ZHANG, Q., GU, X., SINGH, V. P., LIU, L. & KONG, D. 2016. Flood-induced agricultural loss across China and impacts from climate indices. *Global and Planetary Change*, 139, 31-43.
- ZHAO, S., DENG, Y. & BLACK, R. X. 2017. Observed and simulated spring and summer dryness in the United States: The impact of the Pacific sea surface temperature and beyond. *Journal of Geophysical Research: Atmospheres*, 122, 12,713-12,731.
- ZHOU, T., SONG, F., LIN, R., CHEN, X. & CHEN, X. 2013. The 2012 North China floods: Explaining

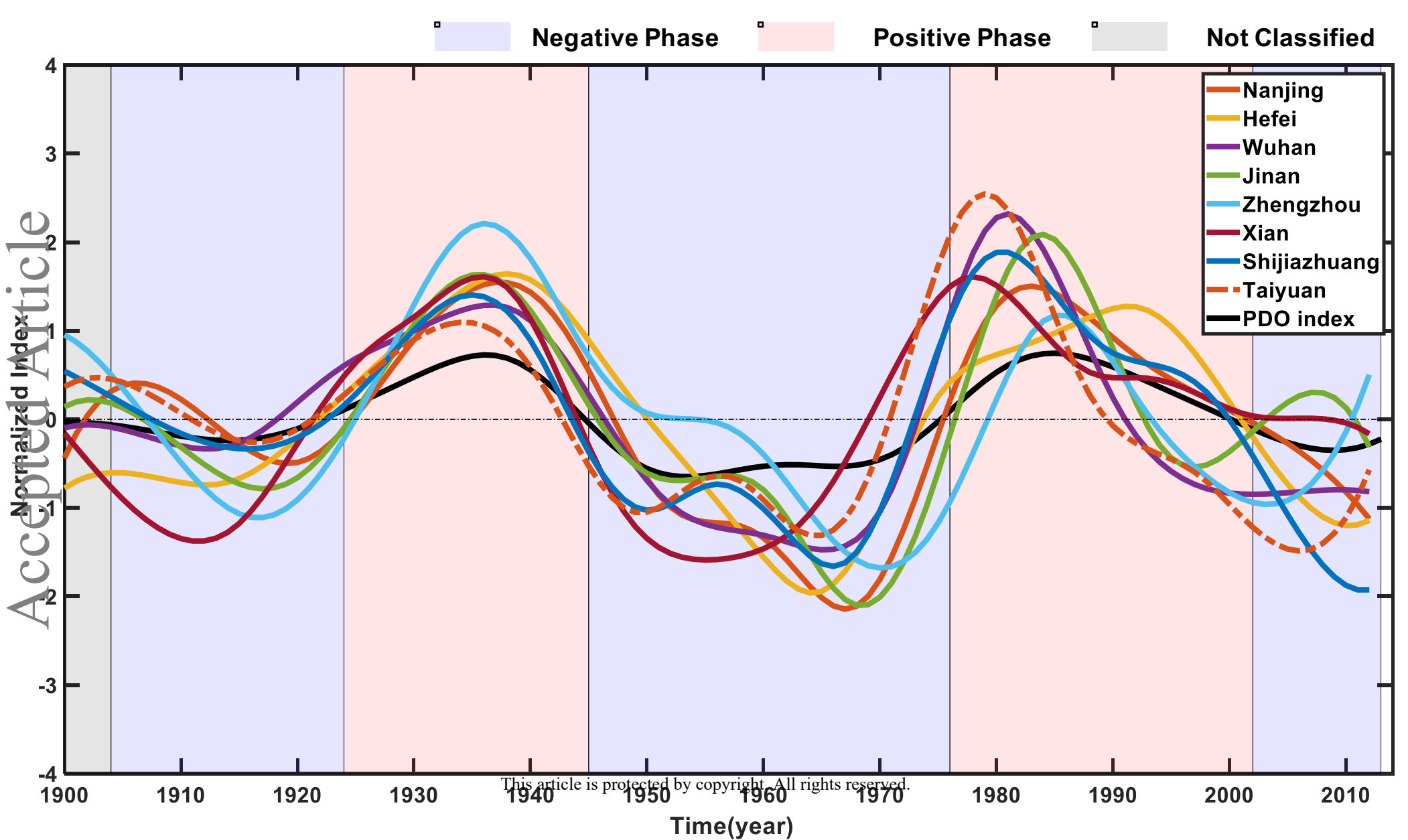
an extreme rainfall event in the context of a long-term drying tendency [in “Explaining Extreme Events of 2012 from a Climate Perspective”]. *Bull. Am. Meteorol. Soc.*, 94, S49-S51.

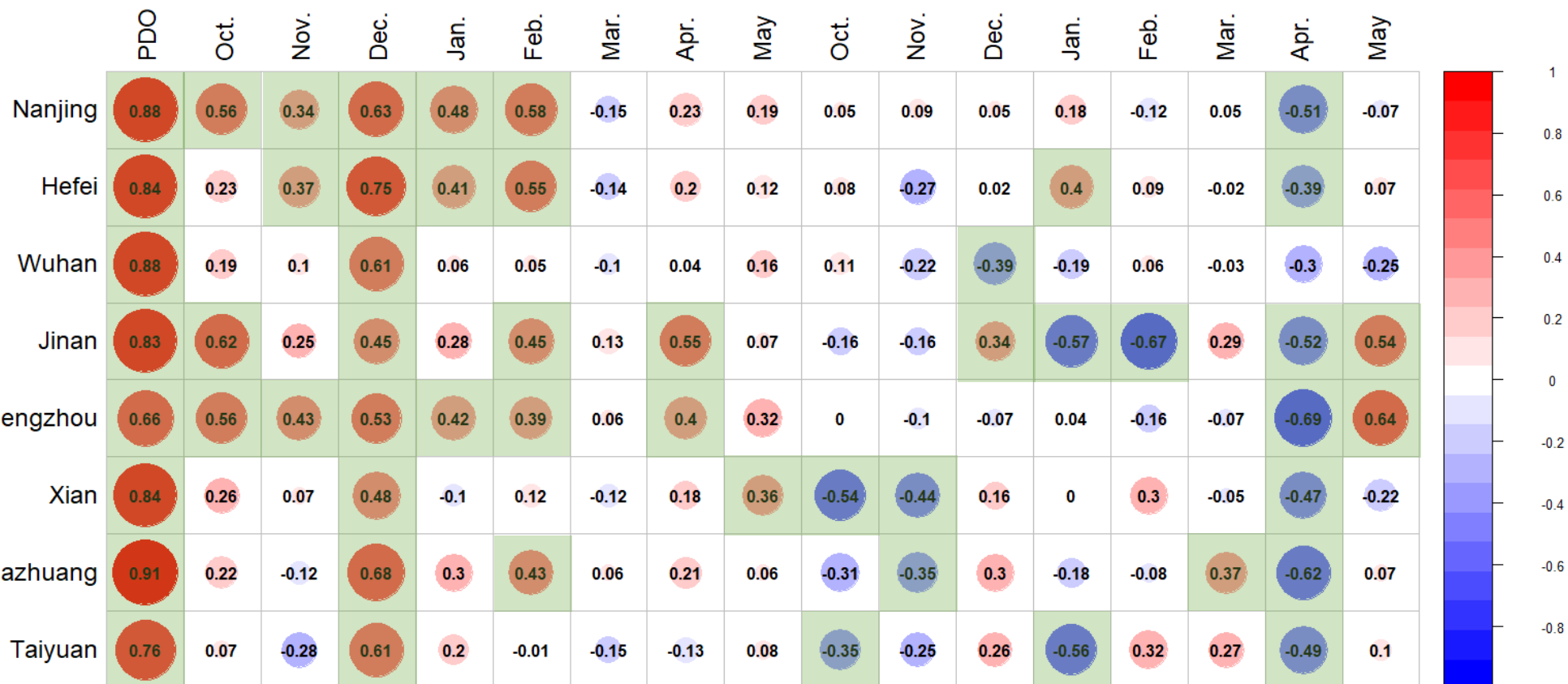












This article is protected by copyright. All rights reserved.

Temperature

Precipitation

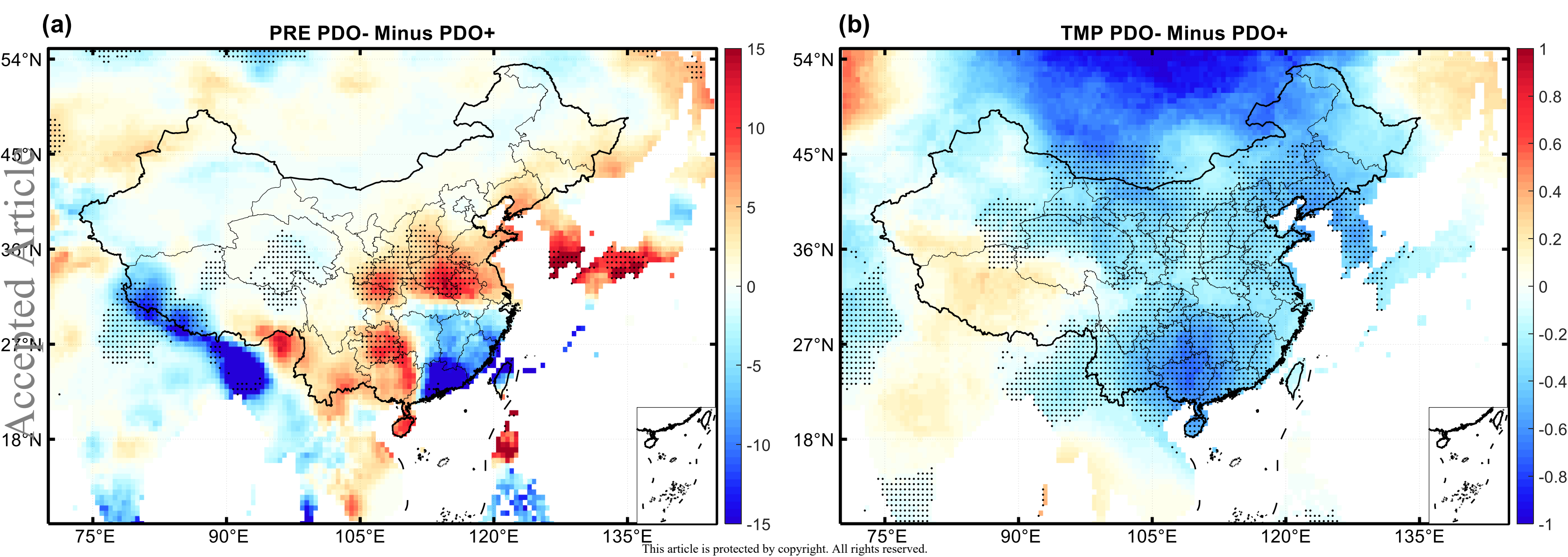


Table 1. Representative location information and genetic coefficients used for the DSSAT model.

Locations	Latitude	Longitude	Sowing date	Genetic coefficients						
				P1V	P1D	P5	G1	G2	G3	PHT
Nanjing	32° 03' N	118° 46' E	20-Oct	51	33	757	24	33	1.2	95
Hefei	31° 51' N	117° 16' E	20-Oct	17	83	425	22	27	1.1	95
Jinan	36° 40' N	117° 00' E	1-Oct	58	59	546	19	22	1.4	95
Wuhan	30° 35' N	114° 17' E	20-Oct	59	43	608	16	29	1.2	95
Zhengzhou	34° 46' N	113° 40' E	1-Oct	19	58	507	16	35	1	95
Xi'an	34° 15' N	108° 55' E	21-Sep	56	79	657	17	21	1.3	95
Shijiazhuang	38° 03' N	114° 26' E	1-Oct	17	36	337	21	22	1.2	95
Taiyuan	37° 51' N	112° 33' E	21-Sep	21	33	649	18	25	1.9	95

P1V, days at optimum vernalizing temperature required to complete vernalization.

P1D, percentage reduction in development rate in a photoperiod hour shorter than the threshold relative to that at the threshold.

P5, grain filling phase duration.

G1, kernel number per unit canopy weight at anthesis.

G2, standard kernel size under optimum conditions.

G3, standard, nonstressed dry weight (total, including grain) of a single tiller at maturity.

PHT, interval between successive leaf tip appearances.

Table 2. The mean periods of various time-scale components for PDO, winter wheat yield, mean temperature and precipitation during 1902–2014 obtained by the EEMD method, respectively.

Partitions	PDO	Yield	Precipitation	Temperature
C1	3.2 yr	2.1 yr	2.9 yr	2.6 yr
C2	8.7 yr	6.7 yr	7.7 yr	7.4 yr
C3	14.1 yr	12.3 yr	14.1 yr	13.5 yr
C4	37.6 yr	31.1 yr	28.5 yr	25 yr
C5	56.5 yr	56.2 yr	56 yr	56 yr